

Structure Evolution of Nanoporous Copper by dealloying of Al 17-33 at% Cu alloy

Yalan Xing¹, Shengbin Wang¹, Baizeng Fang², Shichao zhang^{1,*}, Wenbo Liu¹

¹ School of Materials Science and Engineering, Beihang University, 37 Xueyuan Road, Beijing, China, 100191

² Department of Chemical & Biological Engineering, University of British Columbia, 2360 East Mall, Vancouver, B.C., Canada V6T 1Z3,

*E-mail: csc@buaa.edu.cn

Received: 14 September 2014 / Accepted: 2 April 2015 / Published: 28 April 2015

Three Al-Cu alloys with Cu contents ranging from 17 to 33 at% were prepared by a melt-spun approach, and their dealloying behavior was investigated. After being dealloyed in NaOH solution, the as-produced nanoporous copper (NPC) samples reveal an inherited structure from their precursor alloys in a comparatively large scale, and share similar three-dimensional bicontinuous nanoporous structure in the nano-scale. Some NPCs demonstrate a bimodal size distribution, i.e., macroporous channels (~100 nm) and mesopores (~25 nm). Electrochemical tests reveal the dissolution sequences of different phases in the solution. At elevated temperature, the developed NPC would coarsen into a larger scale.

Keywords: Nanoporous; copper; dealloying; Al-Cu alloy; bimodal pore size distribution

1. INTRODUCTION

Nanoporous metals, featured with high specific surface area, low density and novel chemical properties, have showed great potential in various applications including catalysts [1-3], sensors [4], hydrogen storage [5] and lithium ion batteries [6, 7]. Traditional strategies for preparing nanoporous metals are mainly based on template methods like self-assembled polymer [8], liquid-crystal template [9] and colloidal crystal template [10]. These methods usually involve many steps, such as preparing the template, forming the template-metal composite and removing the template, and therefore are complicated and time-consuming. In contrast, a facile method called dealloying is developed in recent years to prepare unsupported, monolithic, nanoporous bulk metal in one step [11]. Dealloying is a

corrosion process when less noble element is selectively dissolved from an alloy, generating a three dimensional (3D) bi-continuous nanoporous structure [12].

Many alloy systems have been investigated to prepare nanoporous metals through dealloying in the last decade, such as Au-Ag [12-14], Ni-Cu [15], Mn-Cu [16] and Au-Ag-Pt [17]. However, most research focus on uniform nanoporous structures dealloyed from binary/ternary alloy systems with a single solid solution phase. Their research on dealloying mechanism reveal that the activity difference of elements in the solution will lead to the dissolution of less noble element and the rearrangement of more noble element into nanoporous structure. But there have been very few studies on the dissolution competition amongst different phases in an alloy. Al-Cu alloy is a good research object because it could form intermetallics or eutectic structure with different compositions. Zhen Qi et al [18] reported that the Al-Cu alloys with 33 to 50 at% Cu contents in the forms of ribbons, rods, and slices could develop monolithic nanoporous copper (NPC) after being dealloyed. Our group [19] has reported the influence of the phase constituent and the proportion on the formation of NPC from the Al-Cu alloys with a Cu content of 33 to 50 at%.

In this paper, we would discuss the dealloying behavior of Al-Cu alloys with 17 to 33 at% Cu. In this content range, Al and Al₂Cu phases co-exist in the alloys. The structure and morphology relationship between the precursor alloys and the derived NPCs would be discussed. Electrochemical polarization tests were performed to study the activities of the different phases and analyze their dealloying procedures. The coarsening phenomena of NPCs at room temperature (RT) and elevated temperature would be compared to analyze the structure evolution.

2. EXPERIMENTAL SECTION

2.1. Preparation of the Al-Cu alloys and the NPCs

The precursor Al-Cu alloys were prepared by melting pure copper (99.99 wt%) and pure aluminum (99.9%) in a quartz crucibles by voltaic arc heating with the protection of argon atmosphere in designed Cu content (i.e., 17.2, 24.9 and 33.3 at%). These alloys are denoted as Al-17Cu, Al-25Cu and Al-33Cu, respectively for short. The Al-Cu ingots were then processed into slices by melt-spun. The slices are around 50 μm in thickness, 2-5 mm in width and 5 mm -2 cm in length depending on the ductility of the alloy. Dealloying of the Al-Cu alloys was performed in 1M NaOH aqueous solution at RT or elevated temperature for dealloying. Typically, for a dealloyed sample, it would take 5 h till no bubbles could be observed. The samples were then rinsed with distilled water and dehydrated alcohol. After being dried in a vacuum oven, NPCs were obtained.

2.2. Characterization of the Al-Cu alloys and the NPCs

The phase compositions of the Al-Cu alloys and the as-dealloyed NPCs were determined by using X-ray diffraction (XRD, Rigaku D/Max-2400) with Cu K α radiation. Surface morphology and structural analysis were examined by a scanning electron microscopy (FESEM, Hitachi S-4800) with

an energy dispersive X-ray analyzer (EDS), and transmission electron microscopy (TEM, JEOL JEM 2100F).

N₂ adsorption and desorption isotherms were measured at 77 K on a Nova Station A automatic surface area and pore radius distribution apparatus after a sample was degassed at 423 K to 20 mTorr for 12 h. The specific surface areas were determined from the nitrogen adsorption branch using the Brunauer–Emmett–Teller (BET) method. Total pore volumes (V_{Total}) were determined from the amount of gas adsorbed at a relative pressure of 0.99. Pore size distribution (PSD) was calculated from the analysis of the adsorption branch using the Barrett-Joyner-Halenda (BJH) method.

2.3. Electrochemical tests of the different phases

To verify the electrochemical corrosion tendency of different phases in the Al-Cu alloy, potentiodynamic polarization studies were conducted on a single-phase Al metal, Cu metal, Al₂Cu intermetallic compound (i.e. Al-33Cu alloy) and Al-17Cu alloy in 1 M NaOH solution at RT by using an electrochemical measurement unit (PARSTAT 2273). The metal samples were first cut into cubes (1cm×1cm×1cm) and embedded in epoxy resin. An exposed smooth surface was then abraded by sand paper to be tested as working electrode. The experiments were carried out in a standard three-electrode electrochemical cell (200 mL) with a Pt plate electrode as a counter electrode, an Ag/AgCl (sat'd KCl) electrode as a reference electrode. Polarization scan was performed towards positive values at a scan rate of 1.0 mV s⁻¹. The dependence of open circuit potential of Al-17Cu alloy on dealloying time in 1 M NaOH solution at RT was also measured to evaluate the dealloying progress.

3. RESULTS AND DISCUSSION

According to phase-diagram [20], the phase composition of the as-prepared alloys could be predicted. The composition of Al-17Cu lies in the eutectic line. During the solidification, α -Al and intermetallic compound Al₂Cu would precipitate simultaneously from the solution. Al-33Cu has a composition of intermetallic phase, i.e., θ -Al₂Cu. It should be made of pure Al₂Cu. As to Al-25Cu, it falls in the middle of eutectic and intermetallic composition. With the temperature decreasing of the melt, θ -Al₂Cu would first nucleate and grow, and then α -Al and Al₂Cu begin to crystallize together at the eutectic point. The SEM image and EDS spectra of the melt-spun Al-25Cu are shown in Fig.1. There are bright islands with a diameter of 3-10 μ m (denoted as zone A) and dark areas (denoted as zone B) between the islands in the SEM image. The EDS analysis of zone A and B reveal that the atom ratio of Al to Cu in zone A is close to 2:1, which indicates that zone A is a first-solidified θ -Al₂Cu phase. The atom ratio of Al to Cu in zone B is much higher than zone A, implying this area corresponds to an eutectic structure of Al and Al₂Cu that precipitate later in the system. A rapid solidified sample sometimes shows a different structure with equilibrium solidification [21, 22]. Interestingly, in our case, the phase structure is still in agreement with equilibrium conditions except that the grains have smaller sizes.

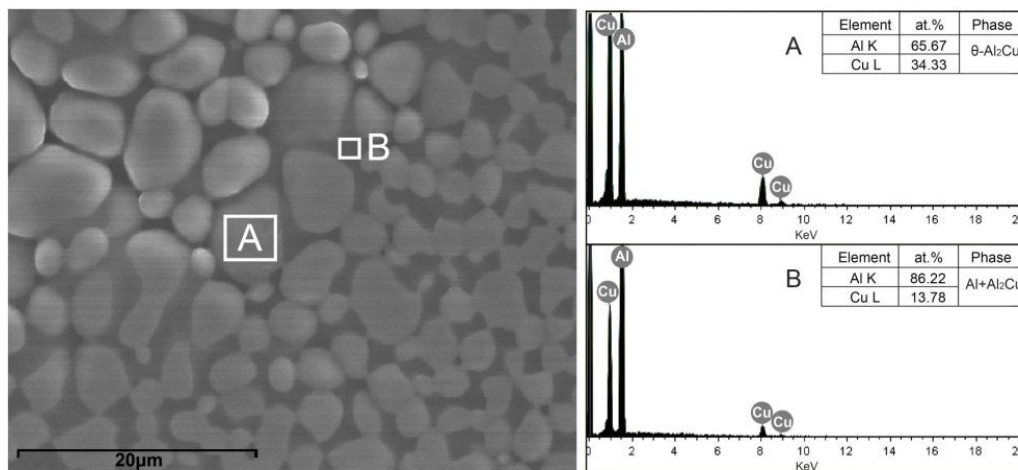


Figure 1. SEM image of alloy Al-25Cu with two feature zones: islands structure (denoted as A) and dark area between islands (denoted as B), and the corresponding EDS analysis results of zone A and B.

Fig. 2 shows the XRD patterns of the precursor Al-Cu alloys. Phase compositions of the alloys vary with the Cu contents. Both Al and Al₂Cu phases were observed in Al-17Cu (Fig. 2a) and Al-25Cu (Fig. 2b), while only Al₂Cu phase exists in the Al-33Cu (Fig. 2c). This result is in accordance with the above metallurgical discussion of alloy structure. Fig. 2d is a typical XRD pattern of dealloyed sample. Though the precursor alloys have different compositions, the obtained NPCs are mainly composed of copper since most Al was dissolved during the dealloying process. But a small peak at ~22 degree indicates that a small amount of residual Al₂Cu exists.

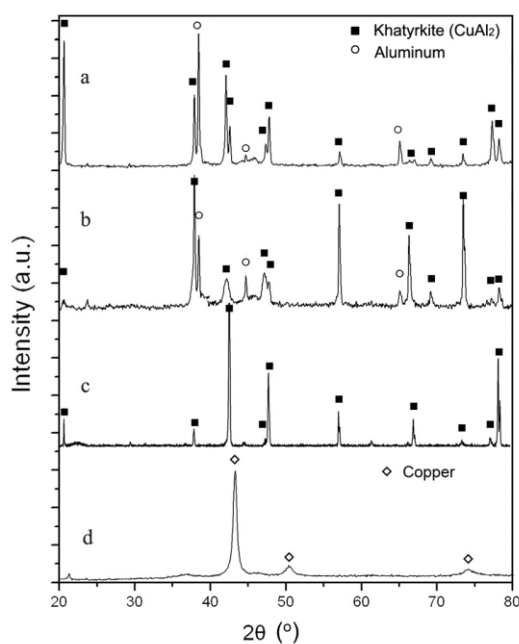


Figure 2. XRD patterns of the precursor Al-Cu alloys (a) Al-17Cu, (b) Al-25Cu, (c) Al-33Cu and (d) a typical pattern of the NPCs derived from the dealloyed Al-Cu alloys.

The nanoporous microstructures of the as-dealloyed NPCs are exhibited in Fig. 3. For the NPC obtained from Al-17Cu alloy, a regular layered structure with smooth channels and walls in a scale of ca. 100 nm was demonstrated. This structure originates from the lamellar structures of the precursor alloys as typical eutectic phases of binary alloys. This lamellar structure is composed of alternating pure Al and Al₂Cu layers. But the Al layers were dissolved while the Al₂Cu layers remained after the dealloying because Al is more active than Cu in the alkaline solution, resulting in the alternating channels/walls structure. The magnified image in Fig. 3(b) displays that the channel walls consist of open, 3D nanoporous structure with pores and ligaments of ca. 20 ~ 30 nanometers in width. This indicates that a typical nanoporous structure is developed on the Al₂Cu layers, implying the Al component in the Al₂Cu layer was also dissolved, leaving voids in the walls. Therefore, the pore distribution of the dealloyed NPCs contains two different scales: the large-sized channels are about 100 nm, while the small-sized pores are about 25 nm. Nanoporous gold (NPG) with similar bimodal pore size distributions has been reported by Zhang et al [23], but the as-prepared NPCs show more ordered large channels with uniform channel size.

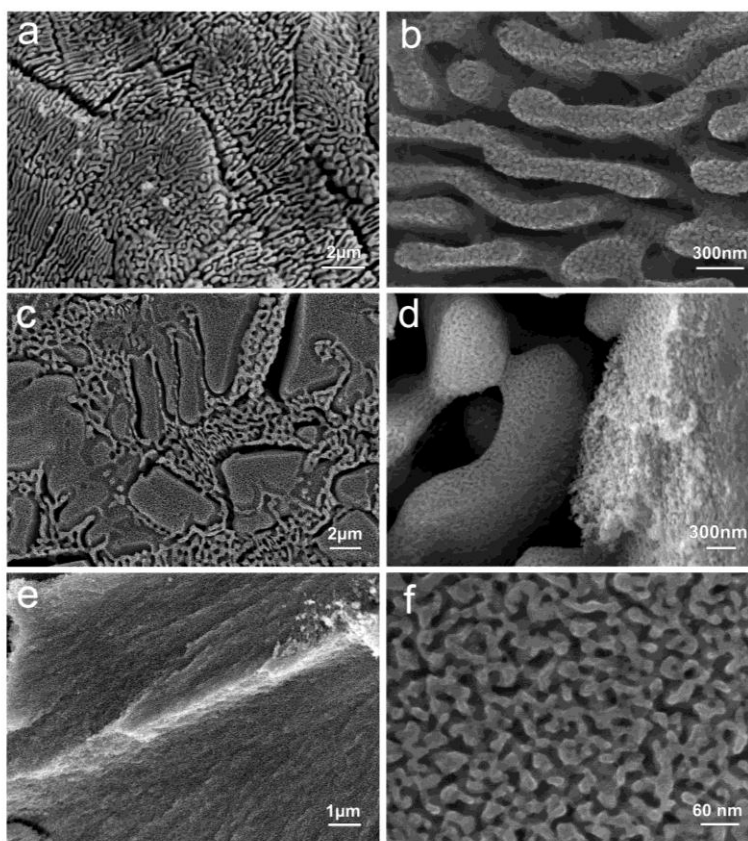


Figure 3. SEM images of the NPCs obtained from (a, b) Al-17Cu, (c,d) Al-25Cu, and (e, f) Al-33Cu after the dealloying at RT.

For the Al-25Cu alloy, the as-dealloyed NPC reveals two characteristic regions, as shown in Fig. 3(c), the island-like region and lamellar region. Compared with Fig.1, the obtained NPC has a similar structure to that of the precursor alloy, indicating that the macroscopic structure is retained

during the dealloying. The island areas are primary Al_2Cu grains while the lamellar structure is simultaneously precipitated Al and Al_2Cu eutectic structure. The magnified image in Fig. 3(d) reveals that both the channel walls in the lamellar structure and the island grains possess 3D nanoporous structure. Similar to Al-17Cu, the Al layer in the lamellar structure and Al element in both Al_2Cu lamellar channel walls and Al_2Cu islands are all dissolved, and nanoporous islands and channel walls are evolved. As for the NPC prepared by the Al-33Cu alloy, it seems more like a plain surface with no lamellar structure, as shown in Fig. 3(e). The high-magnified SEM image in Fig. 3(f) demonstrates that the plane is a uniform structure composed of bicontinuous interpenetrating ligaments and nanopores, which is quite similar to the NPGs reported by Erlebacher [11] and Ding et al [12].

In summary, the structures of the NPCs show an inheritance relationship with their precursor alloys in a comparatively large scale and vary slightly with alloy compositions. Therefore, the large scale structure of the resultant NPCs could be adjusted by controlling the composition and phase structure of the precursor alloys. However, they have similar nanoporous structure in the comparatively small scale no matter in island or lamella, even no matter it is NPC or NPG. During the dealloying of the as-prepared Al-Cu alloy, not only the Al layer in lamellar structure, but also the Al component in the Al_2Cu lamellar channel walls or Al_2Cu islands are dissolved.

For a solid solution alloy system, the dissolution of an element mainly depends on the different electrochemical activity of elements. For a complex alloy system, the dissolution should not only relate with element activity, but also phase activity. To evaluate the corrosion tendency of an element or phase, electrochemical tests were performed. Tafel plots were recorded for the bulk metal samples of single phase Cu, Al, Al_2Cu as well as Al-17Cu alloy, separately. The plots are shown in Fig.4(a) corrosion parameters are listed in table 1. It could be found Al has the most negative corrosion potential (E_{corr}), which is ca. -1.70 V (v.s. Ag/AgCl electrode). Al_2Cu has an E_{corr} of ca. -1.31 V, while Cu is ca. -0.53 V. The phase with more negative corrosion potential has stronger tendency to be dissolved in the solution. Therefore, taking Al-17Cu alloy as an example, when its fresh surface gets contact with alkaline solution, pure Al phase would act as a micro-anode and dissolve in priority. When the corrosion continues, the surface of the alloy changes, and the E_{corr} of the alloy itself would increase. After almost all the Al phase is depleted, the Al_2Cu phase is the most negative one and begins to dissolve. As a result, the Al element in the Al_2Cu is dissolved, while copper goes through the rearrangement to develop NPC structure [11].

Fig.4(b) shows the variation in the open circuit potential (OCP) of Al-17Cu and Al-33Cu alloys as a function of time in 1 M NaOH solution. The curve of Al-17Cu during long-term test could be divided into five stages. At the first stage, the OCP drops rapidly to -1.44V before reaching steady state. During the second stage (12-90 min), the OCP keeps steady and increase smoothly from -1.4V to - 1.3V, corresponding to the dissolution of Al phase since it is corroded as a sacrificial anodic domain. At the end of this stage, the OCP plot gives a fast rise, indicating Al phase is almost depleted and the OCP moves up as anodic current decreasing. From the third stage (90- 170min), it reaches the E_{corr} of Al_2Cu phase, i.e., -1.3V, therefore Al in Al_2Cu start to be corroded. The anodic current is gradually recovered, so the rise of OCP slowed down and show a plateau at around -1.2V. For the forth dealloying stage, the OCP rises steadily toward more anodic value. As Al element in the alloy continuously reduces, the anodic current decreases, and yields higher OCP. However, the OCP shows

some fluctuation in this stage. We assume it is caused by the in-situ rearrangement of Cu elements, which sometimes expose more Al elements underlying. After 280min, the OCP reaches -0.55V and rises very slowly with extended time, indicating the residue is mainly Cu as Al element is depleted.

By comparison, the evolution of the OCP of Al-33Cu alloy (i.e. Al₂Cu) shows some differences. Firstly, the initial steady OCP is around -1.3V, in agreement with its E_{corr} . Furthermore, there is no clear plateau during the rise of the OCP, indicating no new anodic reaction happened during the process.

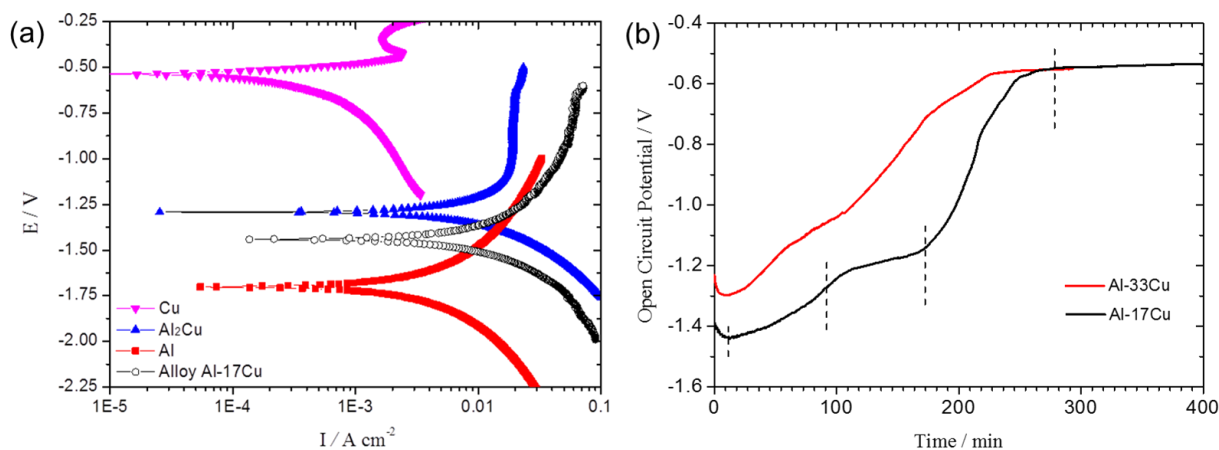


Figure 4. (a) Tafel plots of single phase Cu, Al, Al₂Cu and alloy Al-17Cu and (b) time-dependent evolution of open circuit potential of Al-17Cu and Al-33Cu alloys v.s. Ag/AgCl (sat'd KCl) electrode in 1M NaOH solution.

Table 1. Corrosion parameters of different phases

Phase	E_{corr}	$I_{corr} / 10^{-3} \text{ A cm}^{-2}$
Al	-1.70	8.1
Al ₂ Cu	-1.3	18.1
Cu	-0.53	0.7
Alloy Al-17Cu	-1.44	23.3

The N₂ adsorption/desorption measurements were carried out to study the surface area and porosity of the as-prepared NPC. The isotherms of the NPC obtained from Al-17Cu shown in Fig. 5(a) belongs to a type IV with a H1 hysteresis loop, corresponding to mesoporous solid [24, 25]. The PSD plot in Fig. 5(b) shows a mean mesopore size of ca. 25 nm, which is consistent with the SEM observation. The measurement also reveals that the NPC prepared from Al-17Cu has a BET surface area of ca. 15.5 m² g⁻¹, while the NPC prepared from Al-33Cu shows a little higher surface area (ca. 18.1 m² g⁻¹). Compared with that (i.e., 8.2 m² g⁻¹) of the NPC prepared from Al-15Cu reported by Liu et al [26], the alloy with lower Al content generates NPC with higher surface area. This is because that for an Al-Cu alloy composed of Al and Al₂Cu phases, the phase Al will be depleted to form large channels or voids and contribute little to the surface area of the derived nanoporous material. Al-33Cu,

only consists of Al_2Cu phase, shows the highest surface area among the Al-Cu alloys with Cu content of 0 to 33 at%.

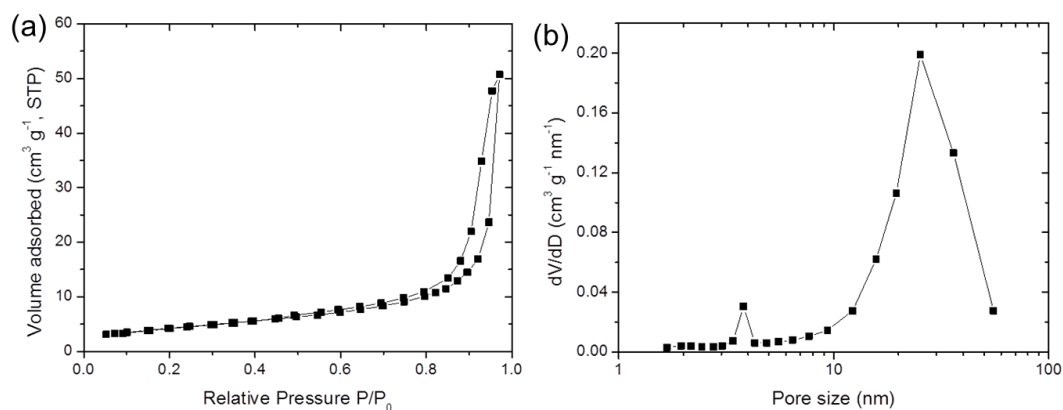


Figure 5. (a) N_2 adsorption and desorption isotherms and (b) Pore size distribution plot based on Barrett-Joiner-Halenda method of NPC prepared from Al-17Cu.

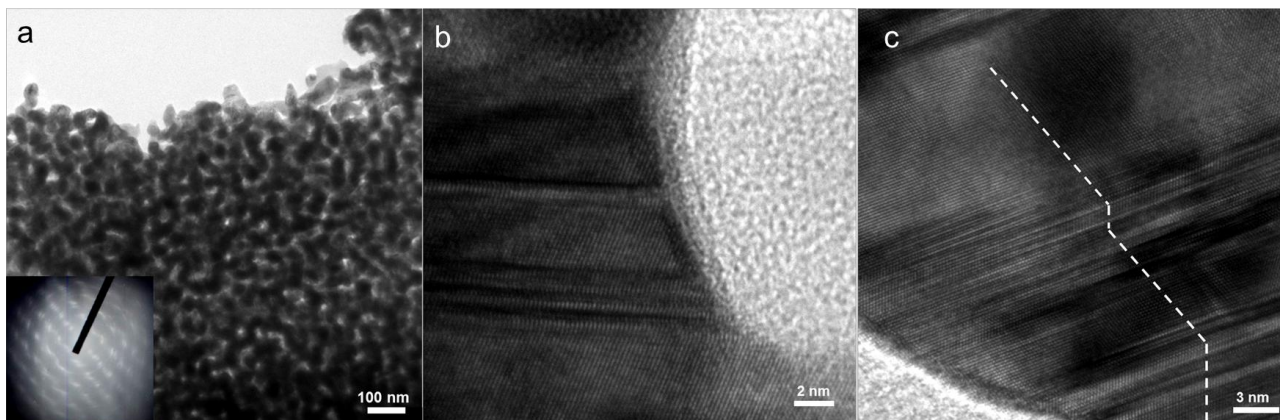


Figure 6. TEM images of the NPC prepared from Al-17Cu. (a) nanoporous structure and its corresponding SAED pattern; HRTEM of a NPC ligament with (b) stacking faults and (c) twins marked by a white dashed line.

Fig. 6(a) reveals the TEM image of the NPC prepared from Al-33Cu. The ligaments could be clearly identified with a width around 20-30 nm. The corresponding selected-area electron diffraction (SAED) pattern inserted in Fig. 6(a) corresponds to face-centered cubic (f.c.c.) Cu along [100] axis. However, the distortion of the diffraction pattern shows a tendency to form diffraction rings, which implies the ligaments are not highly oriented as reported for the NPG prepared from the solid solution Au-Ag alloy [27, 28]. This is probably caused by the different lattice structure between the precursor alloy (Al: f.c.c; Al_2Cu : body centered tetragonal) and the resultant NPC (f.c.c.). Copper atoms evolve into f.c.c. copper ligament from the body centered tetragonal Al_2Cu , and this shift in the lattice structure results in a slight disparity of the final NPC grains. In contrast, both the Au-Ag alloy and the resulted NPG is f.c.c. structure. Its crystal lattice orientation is regarded to be retained after dealloying

as reported. Actually, the NPG prepared from the Al-Au alloy (with an intermetallic of Al_2Au) [23] and the NPC prepared from Al-40Cu [18] showed similar diffraction pattern to that observed in this study. Besides, lattice defects are frequently seen in the resultant NPC. The HRTEM in Fig. 6(b) clearly shows some stacking faults on the ligament. Fig. 6(c) shows the twins as marked by white dashed line. These should be caused by the internal stress originated from the huge mass loss and the volume contraction of alloy and the lattice structure changes.

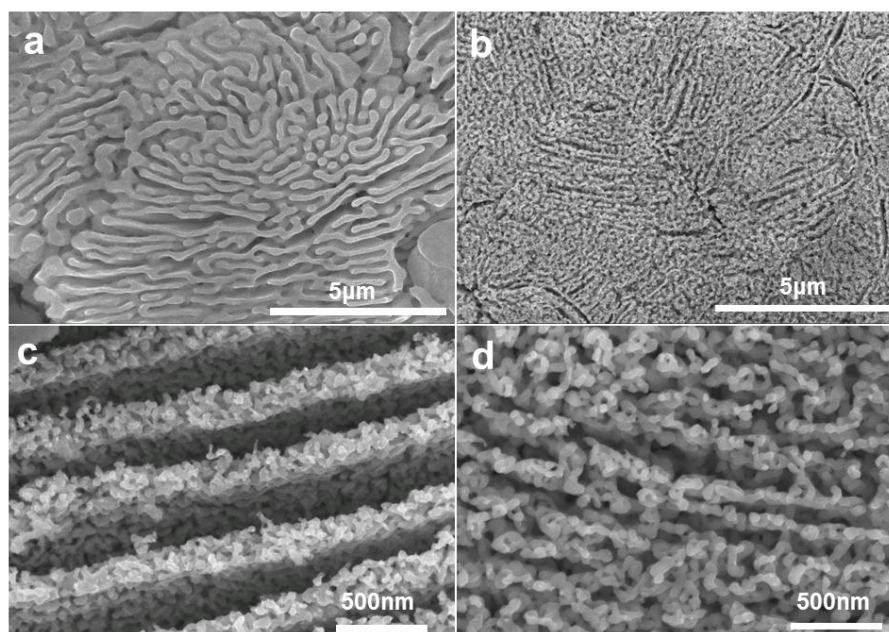


Figure 7. SEM images of the NPC prepared from Al-17Cu alloy at RT (a, c) and 60 °C (b, d) for 5 h, respectively.

Structure coarsening is a widely accepted process accompanying the dealloying reaction, especially at extended time and temperature. The length scale of ligament/nanopores of nanoporous structure formed by more noble metal would coarsen to a larger scale. Fig. 7 displays the NPC images obtained by dealloying Al-17Cu at RT and 60 °C for 5 h, respectively. Comparing the nanoporous structures of Fig. 7 (c) and (d), with the increase in the dealloying temperature, the feature length of the ligaments increases from ca. 25 nm to ca. 50 nm. The NPC prepared from Al-33Cu shows the same length dependence on the dealloying temperature (not shown). Similar phenomena about coarsening have been reported [12, 29], for example, the feature length of the NPG prepared from Au-Ag alloy could be adjusted from ca. 7 nm to ca. 28 nm by tuning the dealloying temperature from -20 to 25 °C. The driving force for such structure evolution is surface-energy reduction, quite similar to Ostwald ripening effect [30]. Dissolution of less noble element will generate ligaments with high curvature composed of more noble metal. The system will try to smoothen regions of high curvature in order to reduce surface-energy, i.e., the atoms will transport from positively curved regions to negatively curved ones [31, 32]. There have been arguments about the evolution mechanism of nanoporous structure between dissolution-redeposition model, volume diffusion model and surface diffusion model

[33]. The prevalent one is the surface diffusion mechanism [11, 34], for which the surface diffusion of more noble metal along alloy/electrolyte interface will be the controlling step. The increase of temperature will enhance the diffusion coefficient, and thus give rise to enlarged length scale of the NPC even dealloyed for the same time as at RT. However, most reports of coarsening are restricted to nano-scale, and it is believed that such coarsening would not lead to long-range mass transport. In our case, the NPC with bimodal pore size distributions shows macroscopic morphology changes at higher temperature. By the comparison of Fig. 7(a) and (b), it could be found the channel/walls eutectic structure in the scale of 100 nm becomes vague for the NPC obtained at 60 °C. The channels are bridged to some extent as shown in Fig. 7(d), which indicates the diffusion of copper has proceeded to the scale of 100 nm. For such alloy system, the coarsening process could be utilized to modify both the microscopic and macroscopic structures.

4. CONCLUSIONS

Three samples of Al-Cu alloy with 17-33 at% Cu were prepared by melt-spun to study their dealloying behavior. Both Al-17Cu and Al-25Cu are composed of α -Al and Al₂Cu, while Al-33Cu is pure Al₂Cu. Their metallographic structure is in accordance with equilibrium solidification analysis except with smaller grain sizes. The resultant NPC after being dealloyed in 1 M NaOH solution at RT shows an inherited structure from the precursor alloy in comparatively large scale and varies slightly with the alloy composition.

Electrochemical tests indicate the different electrochemical activity of Al and Al₂Cu phases and Al is prone to be dealloyed preferentially. The evolution of OCP of Al-17Cu alloy shows a plateau around -1.2V, further reveal that the dealloying of Al₂Cu mainly comes after the Al phase depleted. For the dealloying at elevated temperature, not only the nanoporous structure coarsens into larger scale (ca. 50 nm), but channels/lamellar structure are bridged to some extent.

The prepared NPC by dealloying of Al-Cu alloy possesses bimodal pore size distribution. Its large scaled structure could be altered by controlling the starting alloy composition and phase structure. Its nanoporous structure could be tuned by changing dealloying conditions like temperature or corrosion potential. Such porous metal with large channels facilitating solution percolation and mass transport, nanopores generating more active sites and high surface area favoring interface property, has great potential in various applications, including sensors, catalysts supports and actuators.

ACKNOWLEDGEMENTS

This work was supported by the National Basic Research Program of China (973 Program) (2013CB934001), National Natural Science Foundation of China (51074011 and 51274017) and National 863 Program (2011AA11A257).

References

1. S. Tanaka, T. Minato, E. Ito, M. Hara, Y. Kim, Y. Yamamoto, N. Asao, *Chem. Eur. J.* 19 (2013) 11832 – 11836.

2. A. Wittstock, V. Zielasek, J. Biener, C. M. Friend, M. Bäumer, *Science* 327 (2010) 319-322.
3. C. Xu, L. Wang, R. Wang, K. Wang, Y. Zhang, F. Tian, Y. Ding, *Adv. Mater.* 21 (2009) 2165–2169.
4. H. Qiu, L. Xue, G. Ji, G. Zhou, X. Huang, Y. Qu, P. Gao, *Biosens. Bioelectron.* 24 (2009) 3014–3018.
5. M. Hakamada, H. Nakano, T. Furukawa, M. Takahashi, M. Mabuchi, *J. Phys. Chem. C* 114 (2010) 868–873.
6. S. Zhang, Y. Xing, T. Jiang, Z. Du, F. Li, L. He, W. Liu, *J. Power Sources* 196 (2011) 6915–6919.
7. Y. Yu, L. Gu, X. Lang, C. Zhu, T. Fujita, M. Chen, J. Maier, *Adv. Mater.* 23 (2011) 2443–2447.
8. K. Shin, K. A. Leach, J. T. Goldbach, D. H. Kim, J. Y. Jho, M. Tuominen, C. J. Hawker, T. P. Russell, *Nano Lett.* 2 (2002) 933–936.
9. H. Luo, L. Sun, Y. Lu, Y. Yan, *Langmuir* 20 (2004) 10218–10222.
10. P. Jiang, J. Cizeron, J. F. Bertone, V. L. Colvin, *J. Am. Chem. Soc.* 121 (1999) 7957–7958
11. J. Erlebacher, M. J. Aziz, A. Karma, N. Dimitrov, K. Sieradzki, *Nature* 410(2001) 450-453.
12. Y. Ding, Y. J. Kim, J. Erlebacher, *Adv. Mater.* 16 (2004) 1897–1900.
13. L. Qian, Y. Ding, T. Fujita, M. Chen, *Langmuir* 24 (2008) 4426-4429.
14. J. Biener, A. M. Hodge, J. R. Hayes, C. A. Volkert, L. A. Zepeda-Ruiz, A. V. Hamza, F. F. Abraham, *Nano Lett.* 6 (2006) 2379-2382.
15. L. Sun, C. L. Chien, P. C. Searson, *Chem. Mater.* 16 (2004) 3125-3129.
16. U. S. Min, J. C. M. Li, *J. Mater. Res.* 9 (1994) 2878–2883.
17. J. Snyder, P. Asanithi, A. B. Dalton, J. Erlebacher, *Adv. Mater.* 20 (2008) 4883–4886.
18. Z. Qi, C. Zhao, X. Wang, J. Lin, W. Shao, Z. Zhang, X. Bian, *J. Phys. Chem. C* 113 (2009) 6694–6698.
19. W. Liu, S. Zhang, N. Li, J. Zheng, S. An, Y. Xing, *Corros. Sci.* 58 (2012) 133-138.
20. J. L. Murray. The aluminium-copper system. *Int. Met. Rev.* 30 (1985) 211-234.
21. H. Jones, *J. Mater. Sci.* 19 (1984) 1043-1076
22. L. J. Huang, G. Y. Liang, Z. B. Sun, D. C. Wu, *J. Power Sources* 160 (2006) 684–687.
23. Z. Zhang, Y. Wang, Z. Qi, J. Lin, X. Bian, *J. Phys. Chem. C* 113 (2009) 1308–1314.
24. K. S. W. Sing, D. H. Everett, R. A. W. Haul, L. Moscou, R. A. Pierotti, J. Rouquerol, T. Siemieniewska, *Pure Appl. Chem.* 57 (1985) 603–619.
25. B. Fang, J. Kim, M. Kim, J. Yu, *Acc. Chem. Res.* 46 (2013) 1397-1406.
26. W. Liu, S. Zhang, N. Li, J. Zheng, S. An, Y. Xing, *Int. J. Electrochem. Sci.* 7 (2012) 2240–2253.
27. Y. Ding, A. Mathur, M. Chen, J. Erlebacher, *Angew. Chem. Int. Ed.* 44 (2005) 4002–4006.
28. Y. Ding, M. Chen, J. Erlebacher, *J. Am. Chem. Soc.* 126 (2004) 6876-6877.
29. L. H. Qian, M. W. Chen, *Appl. Phys. Lett.* 91 (2007) 0831051-0831053.
30. P. W. Voorhees, *Annu. Rev. Mater. Sci.* 22 (1992) 197-215.
31. S. Parida, D. Kramer, C. A. Volkert, H. Rösner, J. Erlebacher, J. Weissmüller, *Phys. Rev. Lett.* 97 (2006) 0355041-0355044.
32. K. Sieradzki, *J. Electrochem. Soc.* 140 (1993) 2868-2872.
33. A. J. Smith, T. Tran, M. S. Wainwright, *J. Appl. Electrochem.* 29 (1999) 1085-1094.
34. J. Rugolo, J. Erlebacher, K. Sieradzki, *Nat. Mater.* 5 (2006) 946-949.